

The Spectral Index and its Running in Axionic Curvaton

Fuminobu Takahashi*

Department of Physics, Tohoku University, Sendai 980-8578, Japan

Abstract

We show that a sizable running spectral index suggested by the recent SPT data can be explained in the axionic curvaton model with a potential that consists of two sinusoidal contributions of different height and period. We find that the running spectral index is generically given by $dn_s/d\ln k \sim \frac{2\pi}{\Delta N}(n_s - 1)$, where ΔN is the e-folds during one period of modulations. In the string axiverse, axions naturally acquire a mass from multiple contributions, and one of the axions may be responsible for the density perturbations with a sizable running spectral index via the curvaton mechanism. We note that the axionic curvaton model with modulations can also accommodate the red-tilted spectrum with a negligible running, without relying on large-field inflation.

PACS numbers:

* email: fumi@tuhep.phys.tohoku.ac.jp

I. INTRODUCTION

The origin of density perturbations is one of the central issues in cosmology. While the quantum fluctuation of the inflaton is the simplest possibility, there may be many light scalars in nature, which acquire quantum fluctuations extending beyond the horizon during inflation. If so, some of them may give a significant contribution to the observed density perturbations via the curvaton [1–4] (or its variant, e.g. modulated reheating [5, 6]) mechanism. Those models can be constrained or preferred by observations, especially if one finds an extension(s) of the LCDM cosmology such as non-Gaussianity, running spectral index, dark radiation, isocurvature perturbations, and so on.

Interestingly, the recent SPT data gives preference to a large negative running spectral index [7]¹

$$\frac{dn_s}{d\ln k} = -0.024 \pm 0.011 \quad (1)$$

for the CMB (SPT+WMAP7) data alone. The significance increases further if the BAO and H_0 data are included. In a single-field slow-roll inflation models with a featureless potential, the running spectral index is second order in the slow-roll parameters, and therefore it is of order $(n_s - 1)^2 \sim 10^{-3}$. Thus, it is a challenge to explain the observed running, if taken at face value. There have been various proposals. See e.g. Refs. [9–17].

In this letter we consider a curvaton scenario [1–4] in order to explain the observed running spectral index. We consider an axionic curvaton model in which a pseudo Nambu-Goldstone boson plays a role of curvaton. In order to explain the running, we assume that the curvaton potential consists of two sinusoidal contributions of different height and period. It is possible to generate such potential, if the axion mass receives contributions from several instantons, which may be ubiquitous in the string axiverse [18]. As we shall see later, the running spectral index $\alpha \equiv dn_s/d\ln k$ is generically given by

$$\alpha \sim \frac{2\pi}{\Delta N} (n_s - 1), \quad (2)$$

¹ On the other hand, the ACT data [8] does not give preference for any extensions of the LCDM model. The SPT and ACT observations look at different patches of the sky, and hopefully the tension will be resolved by the Planck or future observations.

where ΔN is the e-folding number during one period of the modulations. Thus, the observed spectral index and its running can be naturally explained if $\Delta N = \mathcal{O}(10)$.

The rest of this letter is organized as follows. In Sec. II, we summarize the latest observational results and the prediction of the spectral index and its running in the curvaton scenario. We present our model in Sec. III and show that the observed running can be explained in the axionic curvaton model with repeated modulations. The last section is devoted for discussion and conclusions.

II. SPECTRAL INDEX AND ITS RUNNING

In this section we summarize the latest SPT result and the expression of the spectral index n_s and its running α in terms of the curvaton potential $V(\sigma)$, which will provide us with implications for the curvaton model building.

The scale dependence of primordial curvature perturbations can be parametrized by the spectral index n_s and its running α defined by [19]

$$n_s(k) = \frac{d \ln \Delta_{\mathcal{R}}^2(k)}{d \ln k}, \quad (3)$$

$$\alpha(k) = \frac{dn_s(k)}{d \ln k}, \quad (4)$$

where $\Delta_{\mathcal{R}}^2(k)$ represents a power spectrum of primordial curvature perturbations \mathcal{R}_k , and k is a comoving wave number. For a constant running, the power spectrum is given in the following form,

$$\Delta_{\mathcal{R}}^2(k) = \Delta_{\mathcal{R}}^2(k_0) \left(\frac{k}{k_0} \right)^{n_s(k_0) - 1 + (\alpha/2) \ln \left(\frac{k}{k_0} \right)}. \quad (5)$$

The latest SPT data combined with the WMAP 7yr data give preference to the non-zero running at more than 2σ [7]

$$\alpha = -0.024 \pm 0.011 \quad (6)$$

with $n_s(k_0^{\text{SPT}}) \approx 0.96$ at the SPT pivot scale $k_0^{\text{SPT}} = 0.025 \text{ Mpc}^{-1}$. If we extrapolate the above result to the WMAP pivot scale $k_0^{\text{WMAP}} = 0.002 \text{ Mpc}^{-1}$, the spectral index is

roughly estimated to be $n_s(k_0^{\text{WMAP}}) \approx 1.02 > 1$. Thus, the spectral index changes from blue-tilted to red-tilted as one goes from k_0^{WMAP} to k_0^{SPT} . The e-folding number between the two pivot scales is $\Delta N_{\text{pivot}} = \ln(k_0^{\text{SPT}}/k_0^{\text{WMAP}}) \simeq 2.5$.

In the curvaton scenario, the spectral index and its running can be expressed in terms of the curvaton potential $V(\sigma)$ and the inflation scale [20]:

$$n_s \simeq 1 + 2 \frac{\dot{H}_*}{H_*^2} + \frac{2V''(\sigma_*)}{3H_*^2}, \quad (7)$$

$$\alpha \simeq 2 \frac{\ddot{H}_*}{H_*^3} - 4 \frac{\dot{H}_*^2}{H_*^4} - \frac{4}{3} \frac{\dot{H}_*}{H_*^2} \frac{V''(\sigma_*)}{H_*^2} - \frac{2}{9} \frac{V'(\sigma_*)V'''(\sigma_*)}{H_*^4}, \quad (8)$$

where σ_* and H_* are the curvaton field value and the Hubble parameter when the cosmological scale k exited the horizon during inflation. The prime denotes the derivative with respect to σ .

Let us make a simplifying assumption that the Hubble parameter hardly evolves during inflation, which is justified except for the large-field inflation.² Then, the above expressions can be simplified as

$$n_s \simeq 1 + \frac{2V''(\sigma_*)}{3H_*^2}, \quad (9)$$

$$\alpha \simeq -\frac{2}{9} \frac{V'(\sigma_*)V'''(\sigma_*)}{H_*^4}. \quad (10)$$

In order for n_s to change from $n_s > 1$ to $n_s < 1$, therefore, the curvature of the potential must change its sign from positive to negative as the curvaton evolves. This requires some structure in the curvaton potential. However, if such structure is present only in a limited field range, we would encounter another problem: why cosmological scales exited the horizon just when the curvaton passed the region where the structure exists. This fine-tuning problem can be avoided if the potential has a structure everywhere in the potential. Indeed, Kobayashi and the present author applied this idea to the large-field inflation by adding repeated modulations to the inflaton potential, and showed that the large negative running can be realized without affecting the overall inflaton dynamics [17].

² We note that the following argument can be applied to large-field inflation in a straightforward way.

This should be contrasted to the result of Ref. [16] that the total e-folds of inflation does not exceed about 30 in the presence of large negative running. In the same spirit of Ref. [17], we consider the curvaton potential with modulations in the next section.

III. AXIONIC CURVATON

We consider an axionic curvaton model, in which the curvaton is a pseudo-Nambu-Goldstone boson. The shift symmetry is assumed to be explicitly broken by e.g. non-perturbative effects as in the QCD axion, generating the following potential:

$$V_0(\sigma) = \Lambda_1^4 \left(1 - \cos \left(\frac{\sigma}{f_1} \right) \right). \quad (11)$$

In the following we will focus on $-\pi < \sigma/f_1 < \pi$ without loss of generality. The axionic curvaton has been studied in e.g. Refs. [21–24]. The model has an advantage that the curvaton mass is protected by the (approximate) shift symmetry which enables the curvaton to acquire quantum fluctuations during inflation.³

The curvaton σ acquires quantum fluctuations $\delta\sigma = H_{\text{inf}}/2\pi$ during inflation, which turn into density perturbations after the curvaton dominates the Universe. Unless the initial position is close to the hilltop, the WMAP normalization of density perturbations [25] imposes the following relation,

$$\left(\frac{H_{\text{inf}}}{2\pi\sigma_*} \right)^2 \simeq 2.4 \times 10^{-9}, \quad (12)$$

where H_{inf} is the Hubble parameter during inflation.⁴ Thus, for a given inflation scale H_{inf} , the WMAP normalization determines σ_* , whose typical value is f_1 . Here and in

³ It is possible to generate density perturbations with a red-tilted spectral index and a vanishingly small running, if σ initially sits in the vicinity of the hilltop, without relying on large-field inflation. The hilltop initial condition generically predicts a sizable non-Gaussianity $f_{\text{NL}} = \mathcal{O}(10)$. This enhancement of the non-Gaussianity is due to non-uniform onset of curvaton oscillations [22, 23]. The importance of non-uniform onset of oscillations in the curvaton scenario was first pointed out in Ref. [22] to our knowledge.

⁴ Precisely speaking, it is necessary to take account of the non-uniform onset of oscillations. However it was shown in [22–24] that the predicted density perturbations are close to that in the case of quadratic potential unless the initial position is close to the hilltop.

what follows we assume that the curvaton dominates the Universe at the decay. We shall come back to this issue in Sec. IV.

As we have seen in the previous section, the observed value of the running spectral index indicates that the spectral index is blue at the WMAP pivot scale, and it is red at the SPT pivot scale. Thus, the curvature of the potential must be initially positive and gradually become negative as the curvaton evolves. Furthermore, the deviation of n_s from unity should be comparable to its running.

First let us see that it is impossible with the curvaton potential (11) to generate such sizable running. Using (9), (10) and (11), we obtain

$$n_s - 1 \simeq \frac{2}{3} \frac{\Lambda_1^4}{f_1^2 H_*^2} \cos\left(\frac{\sigma_*}{f_1}\right), \quad (13)$$

$$\alpha \simeq \frac{2}{9} \frac{\Lambda_1^8}{f_1^4 H_*^4} \sin^2\left(\frac{\sigma_*}{f_1}\right). \quad (14)$$

We note that the spectral index changes from red ($n_s < 1$) to blue ($n_s > 1$), but not the other way around. Thus, the running can be only positive, which is also manifest from Eq. (14). In addition, the running is generically of order $(n_s - 1)^2$, therefore it is too small to account for the observed value [7]. This necessitates some modifications to the curvaton potential (11).

Let us add modulations $\delta V(\sigma)$ to the original potential $V_0(\sigma)$:

$$V(\sigma) = V_0(\sigma) + \delta V(\sigma), \quad (15)$$

with

$$\delta V(\sigma) = \Lambda_2^4 \left(1 - \cos\left(\frac{\sigma}{f_2} + \theta\right)\right). \quad (16)$$

The relative phase θ is not relevant for the following analysis, and so, we will set $\theta = 0$. See Fig. 1. Such two contributions can be originated from the axion anomalous couplings with two different gauge fields, and the multiple contributions to the axion mass are considered to be ubiquitous in the string axiverse [18]. Alternatively we may consider a complex scalar field Φ with an approximate global U(1) symmetry broken by non-renormalizable operators. For instance, consider a scalar potential,

$$V(\Phi) = -m_\Phi^2 |\Phi|^2 + \frac{|\Phi|^{2n-2}}{M_*^{2n-6}} + \left(a_n \frac{\Phi^n}{M_*^{n-3}} + a_m \frac{\Phi^m}{M_*^{m-3}} + \text{h.c.}\right) \quad (17)$$

where M_* is a cut-off scale and we assume $n < m$. Then Φ develops a vev at $\langle \Phi \rangle \sim (m_\Phi M_*^{n-3})^{1/(n-2)}$ and the $U(1)$ symmetry gets spontaneously broken. The phase of Φ is a pseudo-Nambu-Goldstone boson and receives two sinusoidal potentials of different height and period from the breaking terms in the parenthesis. Such a scalar potential can be realized in a supersymmetric theory with a discrete (R) symmetry.

For convenience let us introduce two mass scales, $m_i = \Lambda_i^2/f_i$, where i runs over 1, 2. We assume the following hierarchy among the model parameters [17],

$$m_1^2 f_1^2 \gg m_2^2 f_2^2, \quad (18)$$

$$m_1^2 f_1 \gg m_2^2 f_2, \quad (19)$$

$$m_1^2 \ll m_2^2, \quad (20)$$

which imply $f_1 \gg f_2$. The first two conditions ensure the curvaton dynamics is basically determined by V_0 for most of the field range except for the vicinity of the extrema of V_0 . On the other hand, the third condition tells us that the local curvature of the potential is dictated by the modulations, δV .⁵ In particular, the WMAP normalization condition (12) is maintained, while the spectral index and its running can be significantly affected by the modulations δV .

Let us now derive conditions on the modulations δV to realize the observed spectral index and the running. From (7) and (20), the curvature of δV should satisfy

$$m_2^2 \cos\left(\frac{\sigma_*}{f_2}\right) \simeq \pm \mathcal{O}(0.01) H_{\text{inf}}^2 \quad (21)$$

in order to realize $n_s - 1 = \pm \mathcal{O}(0.01)$ at the SPT and WMAP pivot scales. On the other hand, the slow-roll condition reads

$$m_2^2 \lesssim \mathcal{O}(0.1) H_{\text{inf}}^2. \quad (22)$$

⁵ Apart from the running spectral index, such a set-up will be useful when we would like to realize a red-tilted spectral index in curvaton scenario without relying on large-field inflation which necessitates super-Planckian variation of the inflaton. The modulation generates a red-tilted spectrum, while it is V_0 that determines the curvaton abundance.

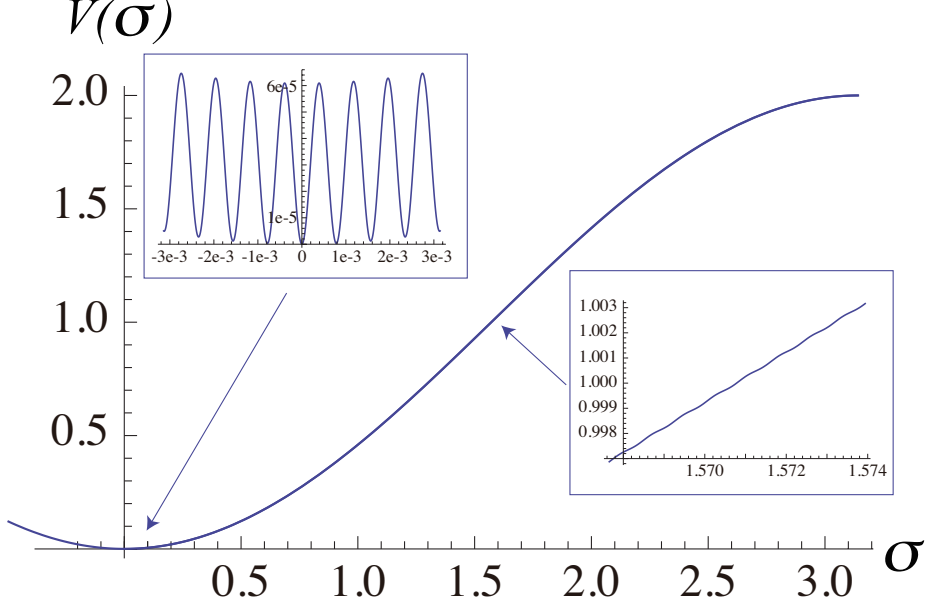


FIG. 1: The potential $V(\sigma)$ is shown. We set $m_1 = 0.01H_*$, $m_2 = 0.44H_*$, and $f_2 = 1.25 \times 10^{-4}f_1$, and the potential and the curvaton field are normalized by $m_1^2 f_1^2$ and f_1 , respectively. We can see the modulations δV is subdominant around the inflection point, but it becomes significant around the origin.

The above two conditions imply

$$m_2^2 \simeq \mathcal{O}(0.1) H_{\text{inf}}^2, \quad (23)$$

$$\cos\left(\frac{\sigma_*}{f_2}\right) \simeq \pm \mathcal{O}(0.1). \quad (24)$$

Furthermore, since the spectral index changes its sign between the two pivot scales, the curvaton should vary by about cf_2 with $c = 0.1 \sim 1$ during the e-folds $\Delta N_{\text{pivot}} \simeq 2.5$.

Let us evaluate the variation of the curvaton $\Delta\sigma$ while the two pivot scales exited the horizon during inflation. The equation of motion can be approximated as

$$3H_{\text{inf}}\dot{\sigma} \simeq -m_1^2 f_1 \sin\left(\frac{\sigma}{f_1}\right), \quad (25)$$

where the dot denotes the derivative with respect to time. Since we are interested in the variation of $|\Delta\sigma| \lesssim f_2 \ll f_1$, we may approximate the rhs of (25) to be a constant. Thus,

$\Delta\sigma$ is related to the increase of the e-folding number ΔN_{pivot} as

$$\Delta\sigma \simeq -\frac{m_1^2 f_1}{3H_{\text{inf}}^2} \sin\left(\frac{\sigma_*}{f_1}\right) \Delta N_{\text{pivot}}. \quad (26)$$

Combined with $\Delta\sigma = cf_2$, we obtain

$$\frac{m_1^2 f_1}{3H_{\text{inf}}^2} \sin\left(\frac{\sigma_*}{f_1}\right) \Delta N_{\text{pivot}} = cf_2 \quad (27)$$

with $c \approx 0.1 - 1$.

The decay constant f_2 determines the period of the modulations. Both the spectral index and its running return to its original value as the curvaton varies by $2\pi f_2$. (Here we have neglected the change of V_0 during one period, because $f_1 \gg f_2$.) As the SPT (and WMAP) data implies an almost constant running over the observed CMB scales, the curvaton should not vary by more than the half of the period πf_2 while the CMB scales exited the horizon. The corresponding e-folding number is roughly $\Delta N_{\text{CMB}} \simeq \ln(\ell_{\text{max}}) \simeq 8$, where $\ell_{\text{max}} \approx 3000$ for the SPT data. Using (26), this constraint reads

$$\frac{m_1^2 f_1}{3H_{\text{inf}}^2} \sin\left(\frac{\sigma_*}{f_1}\right) \Delta N_{\text{CMB}} < \pi f_2, \quad (28)$$

which can be satisfied for f_2 given by (27).

Let us write the spectral index and the running in terms of the curvaton potential. The spectral index is

$$n_s - 1 \simeq \frac{2}{3} \frac{m_2^2}{H_*^2} \cos\left(\frac{\sigma_*}{f_2}\right), \quad (29)$$

and its running is given by

$$\alpha \simeq \frac{2}{9} \frac{m_1^2 f_1 m_2^2}{f_2 H_*^4} \sin\left(\frac{\sigma_*}{f_1}\right) \sin\left(\frac{\sigma_*}{f_2}\right). \quad (30)$$

Thus we can see that both n_s and α oscillate due to the modulations as the curvaton evolves. In particular, it moves clockwise along an oval in the (n_s, α) -plane, as shown in Fig. 2. The oscillation amplitudes A_{n_s} and A_α are related as

$$A_\alpha \simeq \frac{c}{\Delta N_{\text{pivot}}} A_{n_s}, \quad (31)$$

where we have used Eq. (27).

Similarly, we can easily show that the oscillation amplitude of the running spectral index is generally related to that of $(n_s - 1)$ as

$$A_\alpha \simeq \frac{2\pi}{\Delta N} A_{n_s}, \quad (32)$$

where ΔN denotes the e-folds during one period of the modulations δV . Schematically we may express this result as

$$\boxed{\alpha \sim \frac{2\pi}{\Delta N} (n_s - 1)} \quad (33)$$

where α and $n_s - 1$ are understood to represent their typical values. The observed spectral index and the running can be explained for $\Delta N = 20 \sim 30$. (The condition (28) requires $\Delta N/2 > \Delta N_{\text{CMB}} \sim 8$.)

We note that there is an upper bound on ΔN as

$$\begin{aligned} \Delta N &= 2\pi f_2 \left(\frac{m_1^2 f_1}{3H_{\text{inf}}^2} \sin \left(\frac{\sigma_*}{f_1} \right) \right)^{-1}, \\ &< \frac{4\pi}{|n_s - 1|} \frac{|\cos \left(\frac{\sigma_*}{f_2} \right)|}{\sin \left(\frac{\sigma_*}{f_1} \right)}. \end{aligned} \quad (34)$$

Therefore, for e.g. $n_s \simeq 0.97$, ΔN is smaller than a few hundred. In other words, α is always larger than of order $(n_s - 1)^2$ in our framework.

Lastly let us present the numerical results. We set $m_1 = 0.01H_*$, $m_2 = 0.44H_*$, and $f_2 = 1.25 \times 10^{-4} f_1$. The WMAP normalization (12) will determine the relation between f_1 and H_* , and so, all the mass scales are determined if one fixes f_1 (or H_*). The following numerical results do not depend on specific values of f_1 . The only assumption is that the curvaton dominates the Universe before the decay. This condition depends on the thermal history of the Universe, especially the reheating temperature, as well as the decay rate and the oscillation amplitude of the curvaton. We will discuss this issue in the next section.

In Fig. 1, we show the potential $V(\sigma) = V_0(\sigma) + \delta V(\sigma)$. We can see that the modulations do not change much the slope of the potential around the inflection point, while they are

significant around the origin. The evolution of the curvaton after the commencement of oscillations are considered to be more complicated than without modulations, which will be discussed in Sec.IV.

The evolution of n_s and α is shown in Fig. 2. As the curvaton evolves, the predicted (n_s, α) moves clockwise along an oval as indicated by the arrow, and it rotates twice during about 50 e-folds, i.e., $\Delta N \simeq 25$. The solid line represents the numerical result, while the dashed line represents the analytic solution (29) and (30). We also show the SPT and WMAP pivot scales by the star and the triangle, respectively. The CMB scales ($\ell \lesssim 3000$) are shown as the thick line. The position of σ_* is set to be around the inflection point of V_0 , but the result is not sensitive to the value of $\cos(\sigma_*/f_1)$ unless it is extremely close to the extrema of V_0 . (Note that the value of $\cos(\sigma_*/f_2)$ determines the position of the CMB scales along the orbit.) The reason why the actual orbit is not a circle is that our analysis relies on the approximation (18) - (20). In particular, $\delta V'$ partially cancels (enhances) V'_0 when the α is negative (positive). This reduces the change of the running if it is negative. We can see from Fig 2 that the orbit is slightly flattened at the bottom and the running is more or less constant over the CMB scales. We can see that the observed spectral index and the running can be indeed realized in our model.

IV. DISCUSSION AND CONCLUSIONS

Let us here discuss the evolution of the curvaton after inflation. When the Hubble parameter H becomes comparable to m_1 , the curvaton starts to oscillate with an amplitude of order f_1 . The modulations δV does not affect this timing even though the curvature of the potential is determined by δV . This was also confirmed by numerical calculations. As the Universe expands, the oscillation energy evolves as non-relativistic matter. The situation changes when the oscillation energy becomes comparable to the height of the modulations $\delta V \sim m_2^2 f_2^2$. The oscillation amplitude at the time is about $(m_2/m_1)f_2$, which is much larger than f_2 , and so, there are many local minima within the oscillation amplitude. Then the curvaton will be trapped by one of those minima, and the oscillation

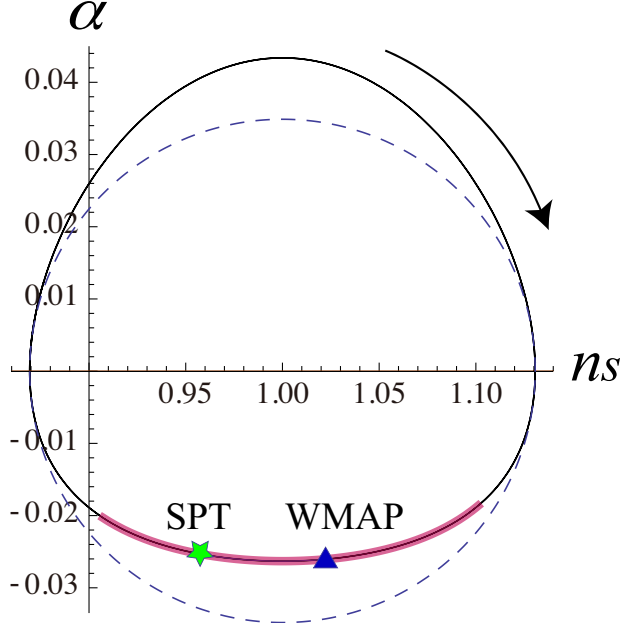


FIG. 2: The evolution of the spectral index n_s and the running α . The numerical result is shown by the solid line, while the dashed line represents the analytic solution (29) and (30). As the curvaton evolves, the predicted (n_s, α) moves clockwise along an oval as indicated by the arrow, and it rotates twice during about 50 e-folds. We also show the SPT and WMAP pivot scales by the star and the triangle, respectively. The CMB scales ($\ell \lesssim 3000$) are shown as the thick line.

(angular) frequency suddenly changes from m_1 to m_2 .

One may expect that domain walls are formed during this transition, because the curvaton will be trapped by different vacuum at different places⁶ Actually however the domain wall formation is hindered by the bias, i.e., the difference in the energy density among those minima, which arises from V_0 . To see this, let us first assume the inflaton-matter dominated Universe. Then the transition takes place when $H_f \sim m_2(f_2/f_1)$. The

⁶ We expect that the curvaton fluctuations with a characteristic frequency are produced through parametric resonance while the curvaton oscillates in a potential with modulations. Then the curvaton oscillations may be spatially inhomogeneous at subhorizon scales.

bias ϵ between the adjacent vacua will be minimized in the vicinity of the origin as

$$\epsilon \gtrsim m_1^2 f_2^2. \quad (35)$$

If the domain walls are formed, the tension is given by $\sim m_2 f_2^2$. Assuming that the scaling law is achieved soon after the formation, the domain walls annihilate effectively when the force of tension acting on the domain walls becomes comparable to the pressure arising from the bias, i.e., $H_{\text{ann}} \sim m_1(m_1/m_2)$. However we can see that

$$H_f > H_{\text{ann}} \implies m_2^2 f_2^2 \gtrsim m_1^2 f_1, \quad (36)$$

which contradicts with (19). This means that the domain walls are not formed from the beginning because of the large bias in the inflaton-matter domination era. On the other hand, if the reheating is completed at the commencement of oscillations, the above condition is modified as

$$H_f > H_{\text{ann}} \implies m_2^2 f_2^{\frac{2}{5}} \gtrsim m_1^2 f_1^{\frac{2}{5}}, \quad (37)$$

which may be satisfied depending on the parameters. For the parameters adopted in the numerical calculation, this condition is marginally satisfied, and so, the domain walls will annihilate quickly even if they formed. The domain walls may play an important role for another choice of parameters, especially in a more general context of the moduli problem in the string axiverse. We leave this for future work. In any case the domain walls are not likely formed, or even if they are formed, they will soon annihilate in the present case.

After the reheating of the inflaton, the fraction of the curvaton energy density will increase until it decays. In order for the curvaton mechanism to work, the curvaton energy should be sizable at the curvaton decay. The fraction of the curvaton energy should be greater than ~ 0.01 in order not to generate too large non-Gaussianity. This often requires a large inflation scale as well as high reheating temperature. Let us comment on how to realize the curvaton domination. For a fixed inflation scale, the decay constant f_1 is more or less fixed unless we adopt the hilltop initial condition. A smaller m_1 would delay the commencement of oscillations, but in the inflaton-matter domination era, it does not increase

the energy fraction of the curvaton.⁷ Thus, it may be necessary to reduce the curvaton decay rate Γ_σ . If the curvaton has an anomalous coupling to massless gauge bosons with a strength of $1/f_i$, the decay rate is considered to be $\Gamma_\sigma \sim (N_g \alpha^2 / 256 \pi^2) m_2^3 / f_i^2$, where α denotes the gauge coupling constant, and N_g denotes the number of decay modes. The decay rate will be suppressed if the gauge coupling is sufficiently small. Alternatively it is possible that the curvaton decays only into a pair of light fermions through the following interaction,

$$\mathcal{L} \supset m_\psi e^{i\sigma/f_i} \bar{\psi} \psi, \quad (38)$$

where such coupling arises if $\psi_{L(R)}$ is charged under the shift symmetry. Then the decay rate is suppressed by the light fermion mass as $\Gamma_\sigma \sim m_\psi^2 m_2 / f_i^2$, which will help the curvaton to dominate the Universe.

Here we comment on the difference from Ref. [17]. First, we have considered a curvaton model, while the large-field inflation was assumed in [17]. Therefore, the tensor mode tends to be smaller in the present case, although the present scenario can be straightforwardly applied to large-field inflation, which produces the tensor mode within the reach of future experiments. A relation between α and n_s like (33) holds in the case of large-field inflation with modulations, if the correction due to the time evolution of H is taken into account. On the other hand, it is possible to generate large non-Gaussianity in our model if the fraction of the curvaton energy is of $\mathcal{O}(0.01 - 0.1)$ at the decay. One important difference is the ease of model building; for the present scenario to work, we need only two sinusoidal potential of different height and period, which can be easily realized in a usual field theory, and no super-Planckian variation of the scalar field is required.

So far we have focused on the generation of density perturbations with a large running spectral index. In fact we can use the model (15) to generate a red-tilted spectrum $n_s \sim 0.97$ with a negligible running, without relying on large-field inflation.⁸ If there is no structure such as modulations, the red-tilted spectrum implies a sizable (tachyonic) mass of the curvaton. Thus, the curvaton will start to oscillate soon after inflation ends unless

⁷ The fraction of the curvaton energy density increases in the radiation domination for a smaller m_1 .

⁸ Note that the running α is still larger than of order $(n_s - 1)^2$, because of (34).

it initially sits in the vicinity of the hilltop [23]. However, this conclusion can be avoided if we add modulations to the curvaton potential. The red-tilted spectrum $1 - n_s = \mathcal{O}(0.01)$ with a negligible running can be realized if we consider large ΔN (i.e., large f_2) with $m_2^2/H_*^2 = \mathcal{O}(0.01)$. This is because the curvaton dynamics (the onset of oscillations as well as the energy density) is determined by V_0 , while it is the modulations that affect the spectral index and its running.

In this letter we have shown that the sizable running spectral index can be explained in the axionic curvaton model in which the curvaton potential receives two sinusoidal contributions of different height and period. The spectral index and the running are generally related to as Eq. (33), and they are comparable in size for $\Delta N = 20 \sim 30$. Such axions with a potential that consists of multiple contributions may be ubiquitous in the string axiverse.

Acknowledgment

The author is grateful to Takeshi Kobayashi for fruitful discussion in the early stage of this work and for reading the manuscript. The author also thanks Tetsutaro Higaki for useful comments. This work was supported by the Grant-in-Aid for Scientific Research on Innovative Areas (No.24111702, No. 21111006, and No.23104008), Scientific Research (A) (No. 22244030 and No.21244033), and JSPS Grant-in-Aid for Young Scientists (B) (No. 24740135) [FT]. This work was also supported by World Premier International Center Initiative (WPI Program), MEXT, Japan

-
- [1] A. D. Linde and V. F. Mukhanov, Phys. Rev. D **56**, 535 (1997) [arXiv:astro-ph/9610219].
 - [2] K. Enqvist and M. S. Sloth, Nucl. Phys. B **626**, 395 (2002) [arXiv:hep-ph/0109214].
 - [3] D. H. Lyth and D. Wands, Phys. Lett. B **524**, 5 (2002) [arXiv:hep-ph/0110002].
 - [4] T. Moroi and T. Takahashi, Phys. Lett. B **522**, 215 (2001) [Erratum-ibid. B **539**, 303 (2002)] [arXiv:hep-ph/0110096].

- [5] G. Dvali, A. Gruzinov and M. Zaldarriaga, Phys. Rev. D **69**, 023505 (2004) [astro-ph/0303591].
- [6] L. Kofman, astro-ph/0303614.
- [7] Z. Hou, C. L. Reichardt, K. T. Story, B. Follin, R. Keisler, K. A. Aird, B. A. Benson and L. E. Bleem *et al.*, arXiv:1212.6267 [astro-ph.CO].
- [8] J. L. Sievers, R. A. Hlozek, M. R. Nolta, V. Acquaviva, G. E. Addison, P. A. R. Ade, P. Aguirre and M. Amiri *et al.*, arXiv:1301.0824 [astro-ph.CO].
- [9] D. J. H. Chung, G. Shiu and M. Trodden, Phys. Rev. D **68**, 063501 (2003) [arXiv:astro-ph/0305193].
- [10] J. M. Cline and L. Hoi, JCAP **0606**, 007 (2006) [arXiv:astro-ph/0603403].
- [11] J. R. Espinosa, arXiv:hep-ph/0605150.
- [12] M. Joy, V. Sahni and A. A. Starobinsky, Phys. Rev. D **77**, 023514 (2008) [arXiv:0711.1585 [astro-ph]].
- [13] M. Joy, A. Shafieloo, V. Sahni and A. A. Starobinsky, JCAP **0906**, 028 (2009) [arXiv:0807.3334 [astro-ph]].
- [14] M. Kawasaki, M. Yamaguchi and J. Yokoyama, Phys. Rev. D **68**, 023508 (2003) [arXiv:hep-ph/0304161].
- [15] M. Yamaguchi and J. Yokoyama, Phys. Rev. D **68**, 123520 (2003) [arXiv:hep-ph/0307373].
- [16] R. Easther and H. Peiris, JCAP **0609**, 010 (2006) [arXiv:astro-ph/0604214].
- [17] T. Kobayashi and F. Takahashi, JCAP **1101**, 026 (2011) [arXiv:1011.3988 [astro-ph.CO]].
- [18] A. Arvanitaki, S. Dimopoulos, S. Dubovsky, N. Kaloper and J. March-Russell, Phys. Rev. D **81**, 123530 (2010) [arXiv:0905.4720 [hep-th]].
- [19] A. Kosowsky and M. S. Turner, Phys. Rev. D **52**, 1739 (1995) [astro-ph/9504071].
- [20] T. Kobayashi and T. Takahashi, JCAP **1206**, 004 (2012) [arXiv:1203.3011 [astro-ph.CO]].
- [21] K. Dimopoulos, D. H. Lyth, A. Notari and A. Riotto, JHEP **0307**, 053 (2003) [hep-ph/0304050].
- [22] M. Kawasaki, K. Nakayama and F. Takahashi, JCAP **0901**, 026 (2009) [arXiv:0810.1585 [hep-ph]].

- [23] M. Kawasaki, T. Kobayashi and F. Takahashi, Phys. Rev. D **84**, 123506 (2011) [arXiv:1107.6011 [astro-ph.CO]].
- [24] M. Kawasaki, T. Kobayashi and F. Takahashi, arXiv:1210.6595 [astro-ph.CO].
- [25] G. Hinshaw, D. Larson, E. Komatsu, D. N. Spergel, C. L. Bennett, J. Dunkley, M. R. Nolta and M. Halpern *et al.*, arXiv:1212.5226 [astro-ph.CO].